



Published in final edited form as:

Mater Horiz. 2017 ; 4(6): 1190–1195. doi:10.1039/c7mh00644f.

Optically Reconfigurable Chiral Microspheres of Self-Organized Helical Superstructures with Handedness Inversion

Ling Wang^a, Dong Chen^b, Karla G. Gutierrez-Cuevas^a, Hari Krishna Bisoyi^a, Jing Fan^b, Rafael S. Zola^d, Guoqiang Li^e, Augustine M. Urbas^c, Timothy J. Bunning^c, David A. Weitz^b, and Quan Li^{a,*}

^aLiquid Crystal Institute and Chemical Physics Interdisciplinary Program, Kent State University, Kent, Ohio 44242, United States

^bSchool of Engineering and Applied Sciences, Harvard University, Cambridge, Massachusetts 02138, United States

^cMaterials and Manufacturing Directorate, Air Force Research Laboratory, Wright-Patterson AFB, Ohio 45433, United States

^dDepartamento de Física, Universidade Tecnológica Federal do Paraná-Apucarana, PR 86812-460, Brazil

^eDepartment of Ophthalmology and Visual Science and Department of Electrical and Computer Engineering, Ohio State University, Columbus, OH 43212, United States

Abstract

Optically reconfigurable monodisperse chiral microspheres of self-organized helical superstructures with dynamic chirality were fabricated via a capillary-based microfluidic technique. Light-driven handedness-invertible transformations between different configurations of microspheres were vividly observed and optically tunable RGB photonic cross-communications among the microspheres were demonstrated.

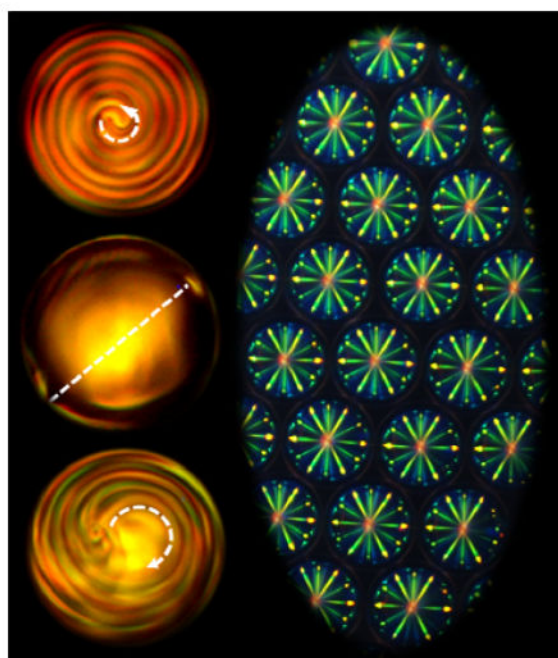
Graphical Abstract

*qli1@kent.edu.

Electronic Supplementary Information (ESI) available: [details of any supplementary information available should be included here].
See DOI: 10.1039/x0xx00000x

Conflicts of interest

There are no conflicts to declare.



Light-driven dynamic structural transformations accompanied by handedness inversion phenomenon were vividly observed in the cholesteric microspheres with low chirality, and optically tunable red, green, and blue (RGB) photonic cross-communications among the microspheres were successfully demonstrated in the systems with high chirality.

Development of stimuli-responsive self-organized supramolecular architectures possessing dynamically reconfigurable properties is currently in limelight due to their great significance in the bottom-up nanofabrication of intelligent miniaturized functional devices such as molecular machines.¹ Light-driven nanoscale chiral molecular switches or motors in liquid crystal (LC) matrix that are able to furnish optically tunable helical superstructures, *i.e.*, photoresponsive cholesteric LCs (CLCs), manifestly represent one such striking system with added advantages of remote, spatial, and temporal controllability.² The helical superstructures of CLCs are characterized by their pitch (P) and handedness. P is the distance along the helical axis when the director completes a 360° rotation, and the direction of twisted molecular orientations determines its handedness.³ Geometric confinement is known to have profound impact on the molecular orientations of liquid crystalline superstructures.⁴ For instance, a polygonal fingerprint texture with light-driven handedness inversion and remarkable stripe rotations was observed in an open film of a photoresponsive CLC placed on a glass substrate treated with a unidirectional alignment layer,⁵ where the collective action of overcrowded alkene-based molecular motors embedded in the CLC matrix was harnessed to controllably rotate microparticles with remote light as the fuel. Interestingly, a well-oriented uniform fingerprint texture was obtained when confining the CLCs in the cells with hybrid-aligned boundary conditions and photoinduced handedness inversion of CLCs was found to facilitate optically rotatable phase gratings with large rotation angle.⁶ Recently, we demonstrated the light-induced, three-dimensional (3D) control over the helical axis of handedness invertible CLCs in the anti-parallelly planar

aligned cells.⁷ Besides these confinements in traditional two-dimensional (2D) flat geometries, confining CLCs into 3D architectures has been envisioned to facilitate the formation of numerous supramolecular configurations with intriguing phenomena and unprecedented functionalities.⁸

Self-organized chiral microspheres, *i.e.*, confining the CLCs into micrometer-sized 3D droplets, have received considerable attentions since it offers new capabilities for emerging applications such as chiral sorting,⁹ omnidirectional lasing,¹⁰ optical vortex generation,¹¹ and photonic cross-communications.¹² With recent advancements in capillary-based microfluidic technique, it has become possible to fabricate monodisperse cholesteric microdroplets with controllable size, shape and morphology.¹³ Optically tunable omnidirectional laser emission has been demonstrated in cholesteric microshells, where the photoresponsive CLCs were formulated by loading photochromic chiral azobenzene switch into achiral LC host.¹⁴ Moreover, light-directed omnidirectional circularly polarized reflection was achieved in microdroplets of photoresponsive CLCs enabled by chiral diarylethene switch and overcrowded alkene based molecular motors.¹⁵ When confined into spherical microdroplets, CLCs are known to adopt diverse equilibrium configurations which result from the delicate interplay between elasticity, chirality, and surface energy.¹⁶ Recent theoretical studies on cholesteric microdroplets have indicated that frustration imparted by the chirality of CLCs plays a significant role in the structure formations and topological transformations among different configurations.¹⁷ However, the experimental investigations on the stimuli-directed transformations of cholesteric microdroplets into distinct configurations are very limited and studies on reversible handedness inversion in CLC microdroplets driven by light stimulus in both forward and backward directions have not been reported.

Light-driven dynamic handedness inversion of CLCs are typically achieved by doping unique light-driven chiral molecular switches or motors into an achiral liquid crystal medium, but rational molecular design of such chiral molecular switches conferring handedness inversion capability to CLCs is not trivial. Therefore, the event of handedness inversion of CLCs driven by light is often encountered by chance.³ Herein, we have designed and synthesized a new photochromic axially chiral azobenzene molecular switch **Azo4** (Figure 1a) that exhibits high compatibility with LC media, high helical twisting power (HTP) and displays large HTP difference between its two photoisomeric states. A photoinsensitive partner **R5011** was judiciously chosen as a codopant owing to its high HTP value and greater solubility in the LC medium (Figure 1b). Light-driven dynamic handedness inversion was accomplished by formulating CLCs containing the new photoresponsive chiral molecular switch **Azo4** and the photoinsensitive chiral dopant **R5011** with opposite chirality (Figure 1c). The selective reflection of the handedness invertible CLC could be facilely tuned from infrared to visible, even ultraviolet regions by appropriately adjusting the relative concentrations of the chiral dopants. Optically reconfigurable monodisperse chiral microdroplets of the resultant self-organized helical superstructures with dynamic handedness inversion capability were fabricated by using a capillary-based microfluidic technique. Interestingly, light-driven structural transformations accompanied by dynamic handedness inversion were accomplished in the CLC

microdroplets with low chirality, *i.e.*, long pitch, whereas optically tunable photonic cross-communications between the droplets were successfully demonstrated in the systems with high chirality, *i.e.*, short pitch. To the best of our knowledge, this is the first time that reversible handedness inversion in CLC microdroplets has been achieved by sole action of light stimulus. This study opens up new routes for understanding the reconfigurable aspects of handedness invertible CLC microspheres. Furthermore, such light-driven dynamically reconfigurable self-organized 3D photonic superstructures may find applications in advanced optical and photonic devices as well as next-generation communication systems.

The novel light-driven nanoscale axially chiral azobenzene molecular switch **Azo4** containing two semiflexible rod-like moieties was prepared by a straightforward synthetic route, and its identity was established by ^1H and ^{13}C NMR spectroscopy, and elemental analysis (see Supplementary Information). The photoswitchable behaviors of **Azo4** and **Azo4-R5011** mixture in CH_2Cl_2 were ascertained by recording UV-vis absorption and circular dichroism (CD) spectra (Figure S1 and S2). The switch **Azo4** was found to exhibit high solubility (as high as 15 wt%) and high HTP value (Figure S4) in a commercially available achiral nematic host SLC1717 (Slichem Liquid Crystal Material Co., Ltd, $T_{N-I} = 91.8\text{ }^\circ\text{C}$, $n = 0.22$, $\epsilon = 12.2$ at 298 K). To explore the photoresponsive behaviors of **Azo4** in LC media, CLC mixtures loaded with **Azo4** were capillary-filled into the planar cells (10 μm cell-gap, antiparallel rubbing alignment) which were painted black on one side. Figure 2a shows the ultra-wide colorful reflection distribution of cholesteric thin film with gradient concentrations of chiral switch **Azo4** confined in a single planar LC cell, taken from a polarized optical microscope (POM) with crossed polarizers. Deep ultraviolet reflections were enabled by high doping concentration of **Azo4** (Figure 2a, right), while far infrared reflections were obtained with low chiral concentration (Figure 2a, left). Figure 2b and 2c indicates the reflection color variations of the CLCs doped with 7 wt % **Azo4** in SLC1717 at room temperature under the UV (365 nm, 30 mW/cm^2) and visible light (460 nm, 30 mW/cm^2) irradiations, respectively. Notably, reversible light-directed RGB reflection colors were achieved in a single cell. Upon UV irradiation at 365 nm, the reflection wavelength was found to red-shift to ~ 500 nm in only 30 s and the system reaches its photostationary state (PSS) in 60 s with a reflection wavelength centered around 580 nm (Figure 2b and 2e). The PSS could be photochemically switched back to a nearly initial state by visible light irradiation at 460 nm within 3 min as shown in Figure 2c and 2f. The photonic reflection colors across the entire visible spectrum were uniform and brilliant, and this reversible tuning of photonic reflection across RGB colors was repeated many times without noticeable degradation. Furthermore, optically addressable RGB patterned display was demonstrated by using light-driven chiral molecular switch **Azo4** (Figure 2d), where the capital alphabets “ABC” with RGB colors were simultaneously written in a single LC thin film by the combination of variable photomasks and different UV irradiation times. The initial dark background came from the deep UV reflection of the CLCs with 8 wt % **Azo4** in SLC1717, and the colorful red “A”, green “B” and blue “C” were facilitated by masking the cell at different areas followed by UV irradiations for certain duration as follows: blue, irradiated for 10 s; green, irradiated for 30 s; red, irradiated for 60 s. After removal of the photomasks, continued UV irradiation drives the background color toward blue, green, and red accompanied by the red-shift of “ABC” colors. It is worth noting that the reverse process

could be achieved through the visible light irradiation for different times (Figure S5) and the cell is rewritable for many times.

To investigate the evolution of structural transformations within the CLC microspheres with handedness inversion under light exposures, we encapsulated the photoresponsive CLCs into microsized spherical droplets by using a glass capillary-based microfluidic device with two tapered cylindrical capillaries coaxially assembled into a square capillary (see Supplementary Information). 10 wt% poly(vinyl alcohol) (PVA) aqueous solution was used to not only surround and stabilize the cholesteric microdroplets against coalescing, but also promote a planar orientation of liquid crystalline molecules at the spherical interfaces thus endowing radial orientation of the helical axes.¹⁸ The resultant spherical cholesteric microdroplets are monodisperse with a diameter of approximately ~ 90 μm . Figure 3 illustrates the real-time changes in POM textures of the microdroplets fabricated from CLCs doped with 1 wt% **Azo4** and 0.4 wt% **R5011** in SLC1717 under the UV illumination. The handedness inversion process of the CLC film in a wedge cell is shown in Figure S6. The low chirality of CLCs, *i.e.*, reduced concentration of chiral dopants, bestowed the cholesteric microdroplets with pitch in the micrometer range which enabled direct observation of the *finger print* under POM. Double spiralized patterns without apparent disclination were initially observed within the microdroplets as shown in Figure 3a, and the counter-clockwise-rotating spirals indicate the left-handedness of CLCs. As the UV irradiation is turned on, the period of spiraling structures gradually increases (Figure 3b–3d) due to the decrease in the chirality of CLCs, and shortly thereafter appears a bipolar nematic configuration (Figure 3e) with two point defects at the poles of the droplets. Continued UV irradiation results in the formations of spherical planar configurations (Figure 3f, 3g) with clockwise-rotating spirals which results from the photoinduced right-handedness of CLCs. The period of spiraling structures steadily decreases (Figure 3h–3j) followed by concentric ring pattern with line defects across the droplets (Figure 3k), and diametrical configuration (Figure 3l) with ring defects arises at the photostationary state. These results vividly demonstrate the photoinduced structural transformations within the CLC microdroplets with dynamically invertible chirality. The underlying mechanism has been schematically illustrated in Figure S9. The occurrence of diverse characteristic patterns in this single dynamic system is unprecedented.

As is well known, selective reflection in visible region could be observed in CLCs with high chirality provided that the periodicity of helical superstructure is in the order of the wavelength of visible light.¹ It is interesting to explore the cooperative photonic interactions between microdroplets by appropriately increasing the chirality of CLCs. Therefore, we fabricated the monodisperse microspheres of CLCs with high chirality and investigated the light-driven dynamic handedness inversion phenomenon, where the CLCs were developed by doping 10 wt% chiral molecular switch **Azo4** and 4 wt% **R5011** in achiral nematic host SLC1717. The handedness inversion process of the CLC film in a planar cell is shown in Figure S6. Figure 4 shows the real-time changes in POM textures of the resultant microdroplets under UV irradiation. Notably, the intriguing multicoloured complex pattern with a bright red central spot surrounded by multiple radial blue lines was observed at the initial state (Figure 4c). The interesting optical pattern is believed to result from the photonic

cross-communications among neighboring microdroplets as schematically demonstrated in Figure 4a. According to Bragg's law, the central wavelength (λ) of reflection is closely related to the helical pitch as $\lambda = nP\cos\vartheta$, where n and P are average refractive index and helical pitch of CLC, while ϑ is the angle between the helix axis and the light propagation direction. When $\vartheta \approx 0^\circ$, *i.e.*, for normal incidence, the light with wavelength of $\lambda = nP$ is reflected from the core of microdroplet as indicated by red arrow in Figure 4a. Due to the curvature of microdroplets, the incident light that hits the periphery as indicated by white arrow would generate a non-zero angle with the helix axes and the light would get reflected with a blue-shifted wavelength. When $\vartheta = 45^\circ$, the light would be reflected from the left microdroplet to the right one as illustrated in Figure 4a (blue arrow). In Figure 4c, the bright red central spot of microdroplets is due to normal reflection at the photonic bandgap wavelength of left-handed CLCs ($\lambda = nP \approx 700$ nm). The appearance of the central spot with normal-incidence reflection also confirms the radial orientation of the CLC helix. The radial blue lines around the central spot arise from the photonic cross-communications with neighboring droplets and this reflection wavelength is determined by $nP\cos 45^\circ \approx 495$ nm. UV irradiations led to the elongation of the helical pitch of CLCs due to the HTP decrease of light-driven nanoscale chiral switch **Azo4**, subsequently causing the red-shift of central and peripheral reflections of microdroplets (Figure 4b, 4d and 4e). Figure 4f and 4g show what happens when the helical pitch is so long that it reflects infrared light, where the appearance of some circular fringes is apparent. When the helical pitch of CLCs keeps increasing and becomes long enough, we could directly observe the internal radial configurations of microdroplets (Figure 4h) under POM with crossed polarizers, where the alternating concentric shells are due to the radial modulation of the index of refraction. The periods of left-handed radial structures increase (Figure 4i) with continued UV irradiations before bipolar nematic configuration (Figure 4j) appears when handedness inversion of CLCs occurs. Further UV irradiation results in the formations of spherical planar configurations (Figure 4k) with clockwise-rotating spirals. As expected, the periods of right-handed spiraling structures steadily decreases (Figure 4l–4o) until the photostationary state was achieved (Figure 4p). Interestingly, the multicoloured complex pattern with a red central spot surrounded by multiple radial green lines could be observed if we keep the sample at the photostationary state for another five minutes (Figure 4q). The red central spot of microdroplets arises from the normal reflection of right-handed CLCs at the photostationary state ($\lambda \approx 750$ nm), and the radial green lines around the central spot result from the photonic cross-communications with their neighbors ($nP\cos 45^\circ \approx 530$ nm). It should be noted that the reverse process could be achieved by visible light (460 nm) irradiation. The light-driven reconfiguration of the microdroplets was repeated many times without noticeable degradation.

In summary, a new photochromic nanoscale axially chiral molecular switch **Azo4** with superior compatibility in achiral LC media was designed and synthesized. The high HTP value of chiral switch in LC matrix and large variation of its HTP value upon light irradiations were harnessed to dynamically tune the reflection colors across the full visible wavelength range in CLCs, which further facilitates optically addressable RGB patterned display. Light-directed dynamic handedness inversion was accomplished in monodisperse CLC microspheres fabricated from an achiral nematic LC codoped with judiciously chosen

photoswitchable left-handed chiral switch **Azo4** and photoinsensitive right-handed chiral dopant **R5011** as partners *via* the capillary-based microfluidic technique. In the low chirality regime, CLC microdroplets exhibited reversible dynamic structural transformations among different topological configurations such as spiral patterns, concentric ring patterns, bipolar and diametrical configurations in a single system upon light irradiations. Interestingly, multicoloured complex patterns from photonic cross-communications between neighboring microdroplets were observed in the high chirality regime. UV irradiations could drive the RGB reflection tuning of colorful cross-communication patterns followed by handedness inversion of cholesteric microdroplets, and reverse process could be achieved through the visible light irradiation or thermal relaxation. The research disclosed here offers a convenient and versatile method to develop the self-organized helical superstructures with programmable handedness inversion capability and stretches the fundamental understanding of the behavior of stimuli-responsive functional soft materials in unconventional and confined geometries. These elegant dynamically reconfigurable self-organized three-dimensional photonic superstructures could find applications in advanced all-optical devices, next-generation communication systems and beyond.

Supplementary Material

Refer to Web version on PubMed Central for supplementary material.

Acknowledgments

Q.Li thanks the support from by the AFOSR and AFRL. G. Li thanks the support from the NIH (through grant R01EY020641) and State of Ohio TVSF fund (through grant TCEG201604).

Notes and references

1. (a) Balzani V, Credi A, Raymo FM, Stoddart JF. *Angew Chem Int Ed.* 2000; 39:3348.(b) Li, Q., editor. *Intelligent Stimuli Responsive Materials: From Well-defined Nanostructures to Applications.* John Wiley & Sons; Hoboken, NJ: 2013. (c) Browne WR, Feringa BL. *Nature Nanotech.* 2006; 1:25.(d) Bisoyi HK, Li Q. *Chem Rev.* 2016; 116:15089. [PubMed: 27936632] (e) Gutierrez-Cuevas KG, Wang L, Zheng Z, Bisoyi HK, Li G, Tan LS, Vaia RA, Li Q. *Angew Chem Int Ed.* 2016; 55:13090.
2. (a) Pieraccini S, Masiero S, Ferrarini A, Spada GP. *Chem Soc Rev.* 2011; 40:258–271. [PubMed: 20938496] (b) Wang Y, Li Q. *Adv Mater.* 2012; 24:1926. [PubMed: 22411073] (c) Zheng Z, Zola RS, Bisoyi HK, Wang L, Li Y, Bunning TJ, Li Q. *Adv Mater.* 2017; 29:1701903.(d) Li Y, Wang M, White TJ, Bunning TJ, Li Q. *Angew Chem Int Ed.* 2013; 52:8925.(e) Bisoyi HK, Li Q. *Acc Chem Res.* 2014; 47:3184. [PubMed: 25181560] (f) Fu D, Li J, Wei J, Guo J. *Soft Matter.* 2015; 11:3034. [PubMed: 25743076] (g) Xie Y, Fu D, Jin O, Zhang H, Wei J, Guo J. *J Mater Chem C.* 2013; 1:7346.
3. (a) Katsonis N, Lacaze E, Ferrarini A. *J Mater Chem.* 2012; 22:7088.(b) Wang L, Dong H, Li Y, Liu R, Wang YF, Bisoyi HK, Sun LD, Yan CH, Li Q. *Adv Mater.* 2015; 27:2065. [PubMed: 25675908] (c) Wang L, Gutierrez-Cuevas KG, Urbas A, Li Q. *Adv Opt Mater.* 2016; 4:247.(d) Bisoyi HK, Li Q. *Angew Chem Int Ed.* 2016; 55:2994.(e) Zhang L, Wang L, Hiremath US, Bisoyi HK, Nair GG, Yelamaggad CV, Urbas AM, Bunning TJ, Li Q. *Adv Mater.* 2017; 29:1700676.(f) Wang L, Bisoyi HK, Zheng Z, Gutierrez-Cuevas KG, Singh G, Kumar S, Bunning TJ, Li Q. *Materials Today.* 2017; 20:230.
4. Crawford, GP., Zumer, S., editors. *Liquid Crystals in Complex Geometries: Formed by Polymer and Porous Networks.* CRC Press; 1996.

5. Eelkema R, Pollard MM, Vicario J, Katsonis N, Ramon BS, Bastiaansen CW, Broer DJ, Feringa BL. *Nature*. 2006; 440:163. [PubMed: 16525460]
6. (a) Lin CH, Chiang RH, Liu SH, Kuo CT, Huang CY. *Opt Express*. 2012; 20:26837. [PubMed: 23187537] (b) Ryabchun A, Bobrovsky A, Stumpe J, Shibaev V. *Adv Opt Mater*. 2015; 3:1273.
7. Zheng ZG, Li Y, Bisoyi HK, Wang L, Bunning TJ, Li Q. *Nature*. 2016; 531:352. [PubMed: 26950601]
8. Wang L, Li Q. *Adv Funct Mater*. 2016; 26:10.
9. Tkachenko G, Brasselet E. *Nature Commun*. 2014; 5:3577. [PubMed: 24717633]
10. (a) Humar M, Mušević I. *Opt Express*. 2010; 18:26995. [PubMed: 21196976] (b) Uchida Y, Takanishi Y, Yamamoto J. *Adv Mater*. 2013; 25:3234. [PubMed: 23637023]
11. Brasselet E, Murazawa N, Misawa H, Juodkazis S. *Phys Rev Lett*. 2009; 103:1039031.
12. (a) Lee SS, Kim SK, Won JC, Kim YH, Kim SH. *Angew Chem Int Ed*. 2015; 54:15266. (b) Noh J, Liang HL, Drevensek-Olenik I, Lagerwall JPF. *J Mater Chem C*. 2014; 2:806. (c) Lee SS, Seo HJ, Kim YH, Kim SH. *Adv Mater*. 2017; 29:1606894.
13. Utada AS, Lorenceau E, Link DR, Kaplan PD, Stone HA, Weitz DA. *Science*. 2005; 308:537. [PubMed: 15845850]
14. Chen L, Li Y, Fan J, Bisoyi HK, Weitz DA, Li Q. *Adv Opt Mater*. 2014; 2:845.
15. (a) Fan J, Li Y, Bisoyi HK, Zola RS, Yang DK, Bunning TJ, Weitz DA, Li Q. *Angew Chem Int Ed*. 2015; 54:216. (b) Aβhoff SJ, Sukas S, Yamaguchi T, Hommersom CA, Le Gac S, Katsonis N. *Sci Rep*. 2015; 5:14183. [PubMed: 26400584]
16. (a) Xu F, Crooker PP. *Phys Rev E*. 1997; 56:6853. (b) Orlova T, Aβhoff SJ, Yamaguchi T, Katsonis N, Brasselet E. *Nature Commun*. 2015; 6:7603. [PubMed: 26145716]
17. (a) Se D, Porenta T, Ravnik M, Žumer S. *Soft Matter*. 2012; 8:11982. (b) Zhou Y, Bukusoglu E, Martínez-González JA, Rahimi M, Roberts TF, Zhang R, Wang X, Abbott NL, de Pablo JJ. *ACS Nano*. 2016; 10:6484. [PubMed: 27249186]
18. Fernández-Nieves A, Vitelli V, Utada AS, Link DR, Márquez M, Nelson DR, Weitz DA. *Phys Rev Lett*. 2007; 99:157801. [PubMed: 17995213]



Figure 1.

Chemical structures of light-driven axially chiral molecular switch **Azo4** (a) and photoinsensitive chiral dopant **R5011** (b). (c) Schematic illustrations of the mechanism of light-driven dynamic handedness inversion in self-organized helical superstructures induced through the doping of **Azo4** and **R5011** with opposite-handedness. At the initial state, the combined doping of two chiral molecules in an achiral nematic LC host yields an overall left handedness which is dominated by that of (*trans, trans*)-**Azo4**. Upon UV irradiation, the left-handed contribution from (*trans, trans*)-**Azo4** decreases significantly due to its *trans-cis* isomerization, while the **R5011** maintains a comparable right-handed contribution with the initial state. When the right handedness becomes dominant, the overall right-handed helical superstructures are achieved.

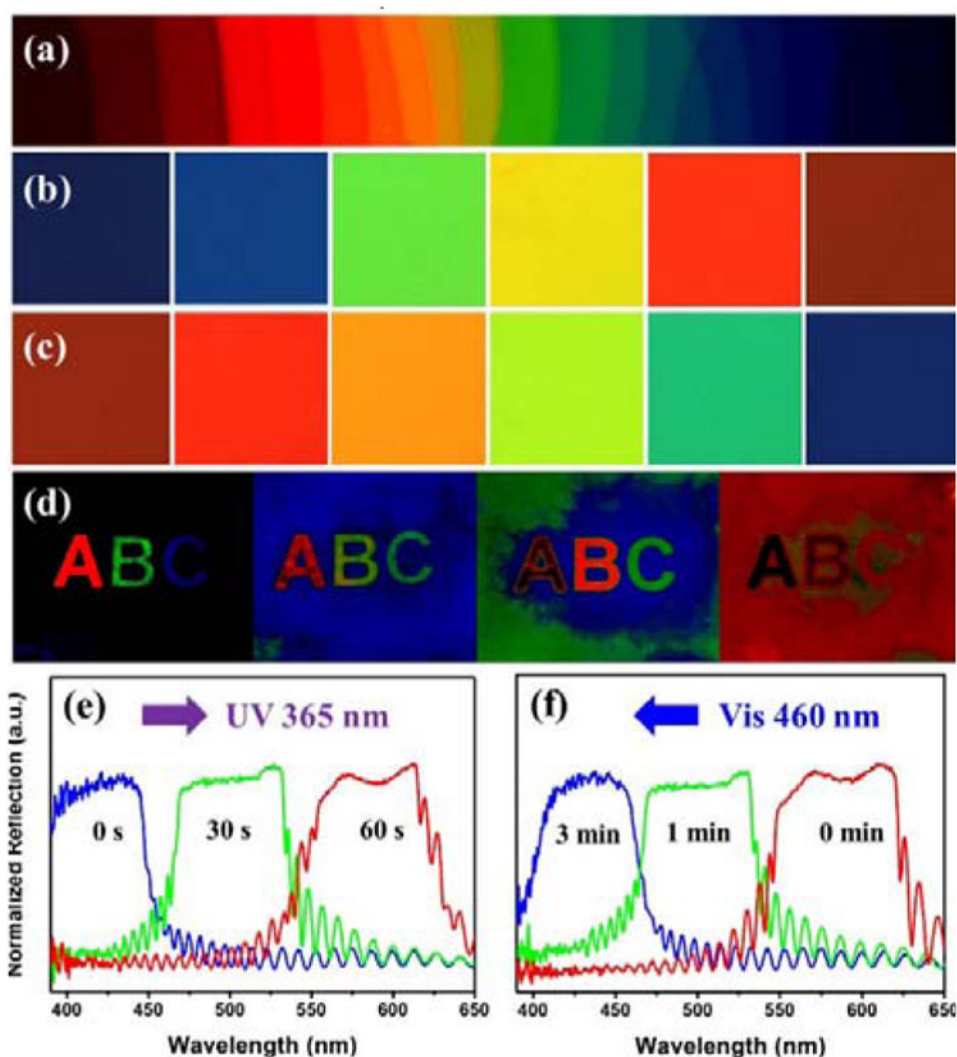


Figure 2. (a) Ultra-wide colorful reflection distribution of CLCs with gradient concentrations of **Azo4** in SLC1717. Reflection colors of the CLCs with 7 wt % chiral switch **Azo4** in SLC1717 at room temperature (b) upon UV irradiation (365 nm, 30 mW/cm²) with different times, and (c) reverse process upon visible irradiation (460 nm, 30 mW/cm²). (d) The real images of a 10 μ m thick CLC film in a planar cell (2.2 cm \times 2.5 cm) filled with 8 wt% **Azo4** in SLC1717 were recorded through the combination of a photomask with the control of UV irradiation time. Reflective spectra of the CLCs with 7 wt % chiral switch **Azo4** in SLC1717 at room temperature (e) under UV light at 365 nm and (f) reverse process upon visible exposure at 460 nm with different times.

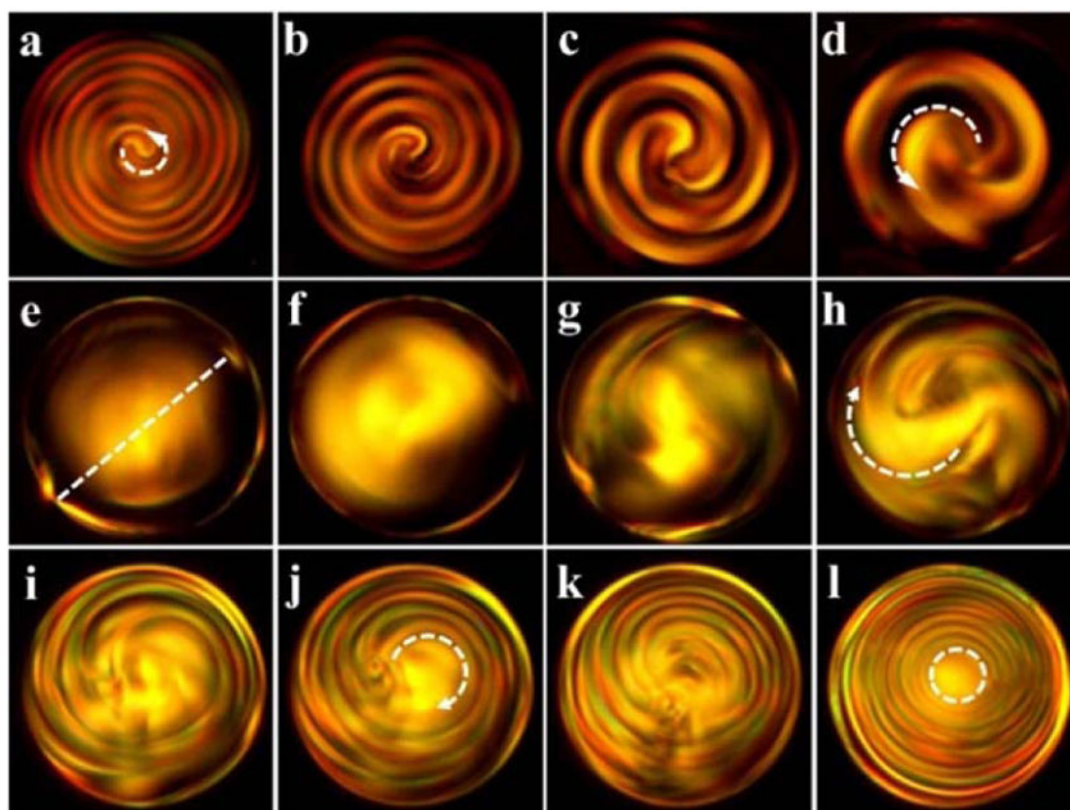


Figure 3.

Real-time changes in microscopic optical textures of the cholesteric microdroplets with low chirality under the UV illumination (365 nm, 15 mW/cm²). Illumination time is 0 s (a), 5 s (b), 15 s (c), 30 s (d), 45 s (e), 60 s (f), 70 s (g), 85 s (h), 90 s (i), 100 s (j), 120 s (k) and 300 s (l), respectively. Notes: anti-clockwise (a, d) and clockwise (h, j) arrows indicate the opposite spirals; dash line (e) connects two point defects at the poles of the droplets and dash ring (l) indicates a ring defect.

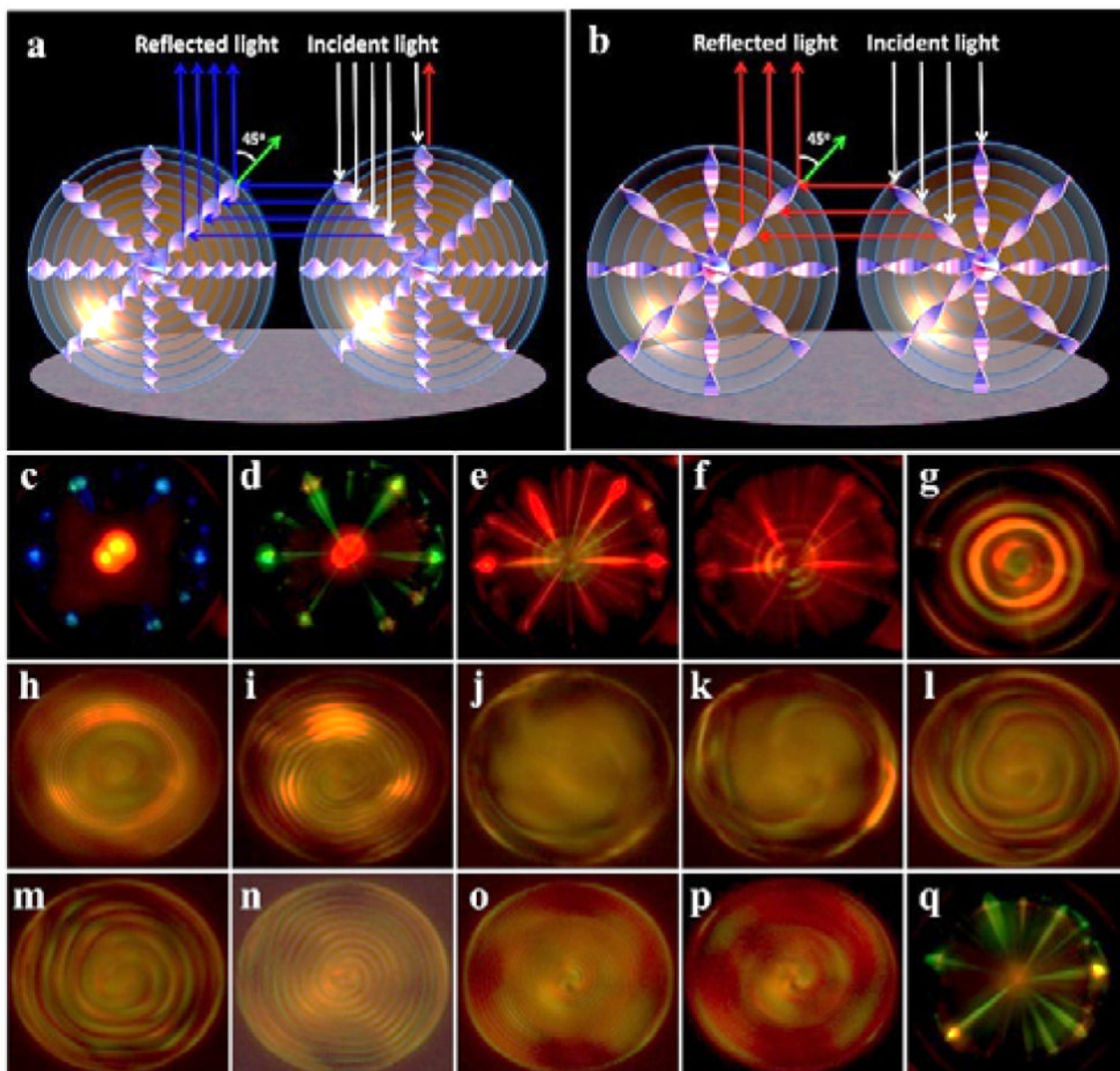


Figure 4. Schematic mechanism of photonic cross-communications between the monodisperse CLC microdroplets with short (a) and long pitch (b), respectively. (c–q) Real-time changes in microscopic optical textures of the microdroplets with high chirality under the UV illumination (365 nm, 10 mW/cm²). Illumination time is 0 s (c), 10 s (d), 20 s (e), 30 s (f), 40 s (g), 60 s (h), 80 s (i), 100 s (j), 110 s (k), 120 s (l), 130 s (m), 150 s (n), 200 s (o), 300 s (p) and 600 s (q), respectively.